Submitted to Optics Communications

UCRL-20394
Preprint

c.2

RECEIVED
LIBRARY
LIBRARY AND
DOCUMENTS SECTION

FAR-INFRARED GENERATION BY PICOSECOND PULSES IN ELECTRO-OPTICAL MATERIALS

J. R. Morris and Y. R. Shen

December 1970

AEC Contract No. W-7405-eng-48

TWO-WEEK LOAN COPY

This is a Library Circulating Copy which may be borrowed for two weeks. For a personal retention copy, call Tech. Info. Division, Ext. 5545

UCRL-20394

LAWRENCE RADIATION LABORATORY
UNIVERSITY of CALIFORNIA BERKELEY

34

DISCLAIMER

This document was prepared as an account of work sponsored by the United States Government. While this document is believed to contain correct information, neither the United States Government nor any agency thereof, nor the Regents of the University of California, nor any of their employees, makes any warranty, express or implied, or assumes any legal responsibility for the accuracy, completeness, or usefulness of any information, apparatus, product, or process disclosed, or represents that its use would not infringe privately owned rights. Reference herein to any specific commercial product, process, or service by its trade name, trademark, manufacturer, or otherwise, does not necessarily constitute or imply its endorsement, recommendation, or favoring by the United States Government or any agency thereof, or the Regents of the University of California. The views and opinions of authors expressed herein do not necessarily state or reflect those of the United States Government or any agency thereof or the Regents of the University of California.

Submitted to Optics Communications

UCRL-20394
Preprint

UNIVERSITY OF CALIFORNIA

Lawrence Radiation Laboratory
Berkeley, California

AEC Contract No. W-7405-eng-48

FAR-INFRARED GENERATION BY PICOSECOND PULSES IN ELECTRO-OPTICAL MATERIALS

J. R. Morris and Y. R. Shen

December 1970

Far-Infrared Generation by Picosecond Pulses in Electro-Optical Materials

J. R. Morris and Y. R. Shen

Department of Physics, University of California
and
Inorganic Materials Research Division,
Lawrence Radiation Laboratory,
Berkeley, California 94720

ABSTRACT

Theoretical calculation of far-infrared power spectra generated by picosecond pulses in a nonlinear optical crystal is presented. Results are illustrated by two practical examples with a $LiNbO_3$ slab oriented for different phase-matching conditions.

Stimulated by a general interest in non-linear optical effects and by the scarcity of powerful sources in the far infrared region, several authors[1-6] have investigated far infrared generation by optical beating in electro-optic materials. Following the development of mode locked lasers with pulse widths in the picosecond range, optical rectification has become a feasible method of generating broadband radiation of high peak power (~ 1 KW), as supported by the recent experimental results.[7] Theoretically, Gustafson et al.[8] have calculated the rectified field for an infinite plane wave in the limit that the optical and far infrared phase velocities differ negligibly. They have also neglected reflection and refraction at the crystal boundaries. This letter reports a more realistic calculation which includes the various effects due to a finite beam cross-section, crystal boundaries, and the significantly different optical and far-infrared phase velocities.

Consider a short laser pulse incident normally on a thin slab of electro-optic material. The slab has a transverse dimension much larger than the beam diameter, and we can assume that the laser pulse propagating in the slab in a single transverse mode is given by[9,10] $\underset{\sim}{E}_\ell = \sum_j \underset{\sim}{E}_{\ell j}(r,t)$ with

$$\underset{\sim}{E}_{\ell j}(\underset{\sim}{r},t) = \underset{\sim}{\mathcal{E}}_{\ell j}\left\{\frac{1}{(1+i\xi_j)}\exp\left[-\frac{x^2+y^2}{w_o^2(1+i\xi_j)} - \frac{(n_j z/c-t)^2}{\sigma^2} + i\,\omega_o(n_j z/c - t) + i\phi\right]\right\} \qquad (1)$$

where w_o is the beam radius in the focal plane, σ is the pulse width,

$\xi_j = (L + z/n_j)/(\omega_o w_o^2/2c)$, L is the distance between the focal point and the front surface of the slab, and z is the distance away from the front surface into the slab. The subindex, j, indicates the polarization state of the laser field. The other quantities have their usual physical meaning.

The laser pulse induces in the slab a nonlinear polarization at difference frequencies of the form

$$\underset{\sim}{P}^{NL}(\underset{\sim}{r},t) = \underset{\approx}{\chi}^{NL} : \underset{\sim}{E}_\ell \underset{\sim}{E}_\ell^{\,*} \tag{2}$$

if we neglect the dispersion of the nonlinear susceptibility $\underset{\approx}{\chi}^{NL}$. The far infrared radiation field $\underset{\sim}{E}(\underset{\sim}{r},t)$ generated in the slab can then be obtained by solving the wave equation

$$[\nabla \times (\nabla \times\ ) + (\underset{\approx}{\varepsilon}/c^2)\frac{\partial^2}{\partial t^2}]\ \underset{\sim}{E}\ (\underset{\sim}{r},t) = -\frac{4\pi}{c^2}\frac{\partial^2}{\partial t^2}\underset{\sim}{P}^{NL}(\underset{\sim}{r},t) \tag{3}$$

with the proper boundary conditions. Here, we have also neglected the dispersion of $\underset{\approx}{\varepsilon}$.

To solve Eq. (3), we use essentially the scheme of Bjorkholm.[10] From the Fourier transform of $\underset{\sim}{E}\ (\underset{\sim}{r},t)$ and $\underset{\sim}{P}^{NL}(\underset{\sim}{r},t)$ on x, y, and t, we obtain the Fourier components $\underset{\sim}{E}\ (\underset{\sim}{k}_T,\omega,z)$ and $\underset{\sim}{P}^{NL}(\underset{\sim}{k}_T,\omega,z)$ respectively. We then use the Green's function method to find $\underset{\sim}{E}(\underset{\sim}{k}_T,\omega,z)$. Although far-infrared radiation is generated in the slab in all directions, only the part which propagates in forward and backward directions with nearly normal incidence on the plane surfaces of the slab can get out of the slab because of the large refractive index of a crystal in the far

infrared. If we are interested only in that part of the far-infrared radiation, then we can use the Green's function for normal incidence as an approximation in finding $\underset{\sim}{E}(\underset{\sim}{k}_T,\omega,z)$. Multiple reflections at the plane boundaries of the slab are clearly important, so that the solution should be proportional to a Fabry-Perot factor. For far-infrared field in the i polarization state, we find at the back surface of the slab, $z = \ell$,

$$\underset{\sim}{E}_i(\underset{\sim}{k}_T,\omega,\ell) = F_i[\underset{\sim}{E}_i^{(S)}(\underset{\sim}{k}_T,\omega,\ z=\ell) - R_i E_i^{(S)}(\underset{\sim}{k}_T,\omega,\ z=0)\ \exp\ (i\omega n_i^{(\omega)}\ell/c)] \qquad (4)$$

with[11]

$$\underset{\sim}{E}_i^{(S)} = (2\pi i\omega/cn_i^{(\omega)}) \int_0^\ell dz'\ \underset{\sim}{P}_i^{NL}(\underset{\sim}{k}_T,\omega,z')\ \exp(i\omega n_i^{(\omega)}|z-z'|/c)$$

where $F_i \cong (1 - R_i)/[1 - R_i^2 \exp(i2\omega n_i^{(\omega)}\ell/c)]$ is the Fabry-Perot factor, and $R_i = (1 - n_i^{(\omega)})/(1+n_i^{(\omega)})$ is the reflection coefficient for the i polarization state.

Experimentally, the far infrared output from the slab is collected by a tapered light pipe leading to a solid-state detector.[12] Since wave propagation in the light pipe has a cutoff angle ϕ_M, the total far infrared power seen by the detector is given by

$$P_i(\omega) = (c/2\pi) \int_0^{|k_T|=(\omega/c)\sin\phi_M} d^2k_T\ |\underset{\sim}{E}_i(\underset{\sim}{k}_T,\omega,\ell)|^2 \cos\phi \qquad (5)$$

where $\phi = \sin^{-1}(k_T c/\omega) \leqslant \phi_m$. To calculate $P_i(\omega)$ from Eq. (5) with the help of Eqs. (1), (2), and (4), we use the following approximations. We assume that the cross-section of the laser beam remains unchanged in traversing the thin slab. If both ordinary and extraordinary laser beams are present, then we also assume that walkoff of the two beams in the slab is negligible. Both assumptions are clearly good approximation when the slab is not unusually thick (< a few mm.). Since ϕ_m is often small, we also approximate $\cos\phi$ by 1 in Eq. (5). Then, if χ^{NL}_{ijk} is the only dominating nonlinear susceptibility in difference-frequency generation, we find, for a slab of thickness ℓ,

$$P_i(\omega) = I_i A |F_i|^2 M_i DS \tag{6}$$

where[13]

$$I_i = (\pi/2C)(\omega\sigma/n_i^{(\omega)})^2 |\chi^{NL}_{ijk}\, \mathcal{E}_{\ell j}\mathcal{E}_{\ell k}/(1+\xi^2)|^2 \ell^2$$

$$A = \pi w_o^2(1+\xi^2)/4, \qquad \xi = \xi_j \ (z=0)$$

$$M_i = |(M^-_{ijk} + M^-_{ikj}) - R_i\ (M^+_{ijk} + M^+_{ikj})|^2$$

$$M^\pm_{ijk} = [1 - \exp\ (i\Delta k^\pm_{jk}\ell)]/i\Delta k^\pm_{jk}\ell$$

$$\Delta k^\pm_{jk} = (1/c)[(\omega_o+\omega/2)n_j^{(\omega_o)} - (\omega_o-\omega/2)n_k^{(\omega_o)} \pm \omega n_i^{(\omega)}]$$

$$D = 1 - \exp[-(\omega^2/4c^2)\ w_o^2(1+\xi^2)\ \sin^2\phi_m]$$

$$S = \exp\ (-\omega^2\sigma^2/4).$$

The various quantities in the above equation have the following physical meanings. A is the effective cross-section of the beam at the slab. $M^{\pm}_{ijk}$ takes care of the phase mismatch in the difference-frequency generation process, with Δk^{-}_{jk} and Δk^{+}_{jk} being the average momentum mismatches for far-infrared waves propagating in the forward and backward directions respectively. D accounts for the diffraction effect due to the finite beam cross-section. S is the spectral content of the picosecond laser pulse. Finally, $I_i A$ gives the far-infrared power spectrum if all the other factors in Eq. (6) are in unity.

We now use Eq. (6) to calculate the spectra of the far-infrared output for two cases. In the first case, a 0.1 cm. $LiNbO_3$ slab is oriented with the c-axis parallel to the plane surfaces of the slab. A 2-psec. laser pulse at 1.06 μ, polarized along the c-axis, is normally incident on the slab, so that χ^{NL}_{33} is the only nonlinear susceptibility responsible for the difference-frequency generation. With $\hat{j} = \hat{k} = \hat{i}$ along $\hat{c}$ and $n_i^{(\omega_o)} \neq n_i^{(\omega)}$ in Eq. (6), phase matching occurs only at $\omega = 0$. The calculated spectrum is shown in Fig. 1. The dashed curve gives the spectrum without the Fabry-Perot boundary condition. The peaks at 5, 8.4, and 11.8 cm^{-1} are the secondary peaks of the phase-matching curve, which would have the major phase-matching peak at $\omega = 0$ if it were not for the low-frequency cutoff. This low-frequency cutoff is mainly due to the ω^2-dependent radiation effects, and gives rise to the first peak at 2 cm^{-1}. The diffraction effect (D) only makes the cutoff even sharper, but does not affect the spectrum significantly beyond the first peak. On the high-frequency side, the spectrum is limited by the spectral content S of the input pulse. With the Fabry-Perot

boundary condition included, the spectrum is then modified by the interference pattern, as shown by the solid curve with spikes in Fig. 1. For an input pulse of 1 - GWatt peak power, the total far-infrared output energy is about 0.1 erg. Our results here agree with those of Gustafson et al.[8] in the limit $n_i^{(\omega)} = n_i^{(\omega_o)}$ and when diffraction and boundary conditions are neglected.

In the second case, the $LiNbO_3$ slab is oriented with the c-axis tilted at 16.8° away from the normal of the slab and the a-axis is in the plane defined by the c-axis and the normal. The normally incident laser pulse is linearly polarized at 45° with respect to the plane such that only χ_{24}^{NL} is responsible for the difference-frequency signal with polarization perpendicular to the plane. We then find from Eq. (6) that the phase-matching conditions $\Delta k_{jk}^{-} = 0$ and $\Delta k_{kj}^{+} = 0$, for far infrared generation in the forward and the backward directions respectively, can be satisfied at $\omega = 15$ and $7.5\ cm^{-1}$ respectively. The far-infrared spectrum is then essentially the superposition of the two phase-matching curves modified by $\omega^2 S(\omega)$ and the boundary conditions. If the boundary conditions are neglected ($R_i = 0$), then only the far infrared generated in the forward direction contributes to the spectrum as represented by the dashed curve in Fig. 2. With the boundary conditions, $R_i \neq 0$, the far infrared generated in the backward direction now appears in the output. Its spectrum dominates over that of the far infrared generated in the forward direction because of the high-frequency cutoff due to $S(\omega)$. The total spectrum is given by the solid curve in Fig. 2, where the spikes are again the result of Fabry-Perot interference. Diffraction has little effect in this

case. For a laser pulse with a 1 - GWatt peak power, the total far-infrared energy generated here is 0.0064 erg. Both cases discussed above have been investigated experimentally. Preliminary results show good agreement with our theoretical calculations.[7]

We have neglected dispersion and absorption in the above discussion. They can, however, be easily incorporated in the computer calculations. The effects vary from crystal to crystal. In $LiNbO_3$, the absorption coefficient, α, in the far infrared is roughly proportional to ω^2. ($\alpha \sim 18\ cm^{-1}$ at $30\ cm^{-1}$).[14] The decrease of the far-infrared power due to absorption is less than 20% below $10\ cm^{-1}$. We have also neglected the effect of possible frequency chirping of a mode-locked pulse.[15] This is not important here since, in the product $E_{\ell j}E^*_{\ell k}$, any phase modulation in $E_{\ell j}$ is almost completely cancelled out by the same phase modulation in $E^*_{\ell k}$. Finally, for a train of N identical mode-locked pulses with a time interval τ between pulses, the far-infrared spectrum should be modified by the factor $|[1 - \exp(iN\omega\tau)]/[1 - \exp(i\omega\tau)]|^2$. The total far-infrared energy is increased by a factor of N.

ACKNOWLEDGEMENTS

This work was performed under the auspices of the U. S. Atomic Energy Commission.

We would like to thank K. H. Yang and P. L. Richards for helpful discussions on the unpublished experimental results.

REFERENCES

1. K. E. Niebuhr, Appl. Phys. Letters 2, 136 (1963).

2. F. Zernike, Phys. Rev. Letters 15, 999 (1965).

3. F. Zernike, Bull. Am. Phys. Soc. 12, 687 (1967).

4. T. Y. Chang, N. Van Tran, and C. K. N. Patel, Appl. Phys. Letters 13, 357 (1968).

5. T. Yajima and K. Inoue, IEEE Journal of Quantum Electronics QE-5, 140 (1969); Phys. Letters 26A, 281 (1968).

6. D. W. Faries, K. A. Gehring, P. L. Richards, and Y. R. Shen, Phys. Rev. 180, 363 (1969).

7. D. W. Faries, P. L. Richards, J. W. Shelton, Y. R. Shen, and K. H. Yang, International Quantum Electronics Conference, Kyoto, Japan, (1970) Paper 8-6; T. Yajima and N. Takeuchi, ibid., Paper 8-5.

8. T. K. Gustafson, J-P. E. Taran, P. L. Kelley, and R. Y. Chiao, Optics Comm. 2, 17 (1970).

9. D. W. Faries, Ph.D. Thesis, University of California, Berkeley, unpublished (1969).

10. J. E. Bjorkholm, Phys. Rev. 142, 126 (1966).

11. For extraordinary far-infrared ray, the equation should be modified to take into account the fact that $\underset{\sim}{E}$ is not perpendicular to $\underset{\sim}{k}$. See J. A. Armstrong, N. Bloembergen, J. Ducuing, and P. S. Pershen, Phys. Rev. 127, 1918 (1962).

12. See, for example, P. L. Richards in "Far Infrared Properties of Solids", edited by S. S. Mitra and S. Nudelman (Plenum Press, New York, 1970), p. 111.

13. For j = k, we should replace I_i by $I_i/4$ if we use the conventional definition for χ^{NL}_{ijj}.

14. D. R. Bosomworth, Appl. Phys. Letters 9, 58 (1966); J. G. Berman, A. Ashkin, A. A. Ballman, J. M. Dziedzic, H. J. Levinstein, and R. G. Smith, Appl. Phys. Letters 12, 92 (1968).

15. E. B. Treacy, Appl. Phys. Letters 17, 14 (1970).

FIGURE CAPTIONS

Fig. 1. The far-infrared spectrum computed from Eq. (6) for a 2 psec. (full width at half-maximum) Nd laser pulse normally incident on a 1-mm. $LiNbO_3$ slab. The crystal is oriented with the c-axis parallel to the plane surfaces of the slab and the laser pulse is polarized along the c-axis ($\chi_{33} = 1.57 \times 10^6$ esu). The other parameters used in the calculation are $w_o = 0.017$ cm. (corresponding to a 4-mrad. divergence of the laser beam), L = 135 cm., $n_i^{(\omega)} = 5.05$ and $n_i^{(\omega_o)} = 2.2$. The solid and the dashed curves are computed with and without boundary conditions respectively.

Fig. 2. The far-infrared spectrum computed from Eq. (6) with the same laser parameters as in Fig. 1. Here, the 1-mm. slab is oriented with the c-axis tilted at 16.8° away from the normal of the slab, and the a-axis is in the plane defined by the c-axis and the normal. The laser is polarized at 45° to the plane, so that only $\chi_{24}^{NL} = 1.54 \times 10^{-6}$ esu is responsible for the difference-frequency signal with polarization perpendicular to the plane. With $\hat{i} = \hat{j}$ (along the b-axis) and $\hat{k}$ being the directions of polarizations of the ordinary and the extraordinary light propagating along $\hat{z}$ respectively, we have $n_i^{(\omega)} = 6.6$, $N_i^{(\omega_o)} = 2.2$, and $n_k^{(\omega_o)} = 2.193$.

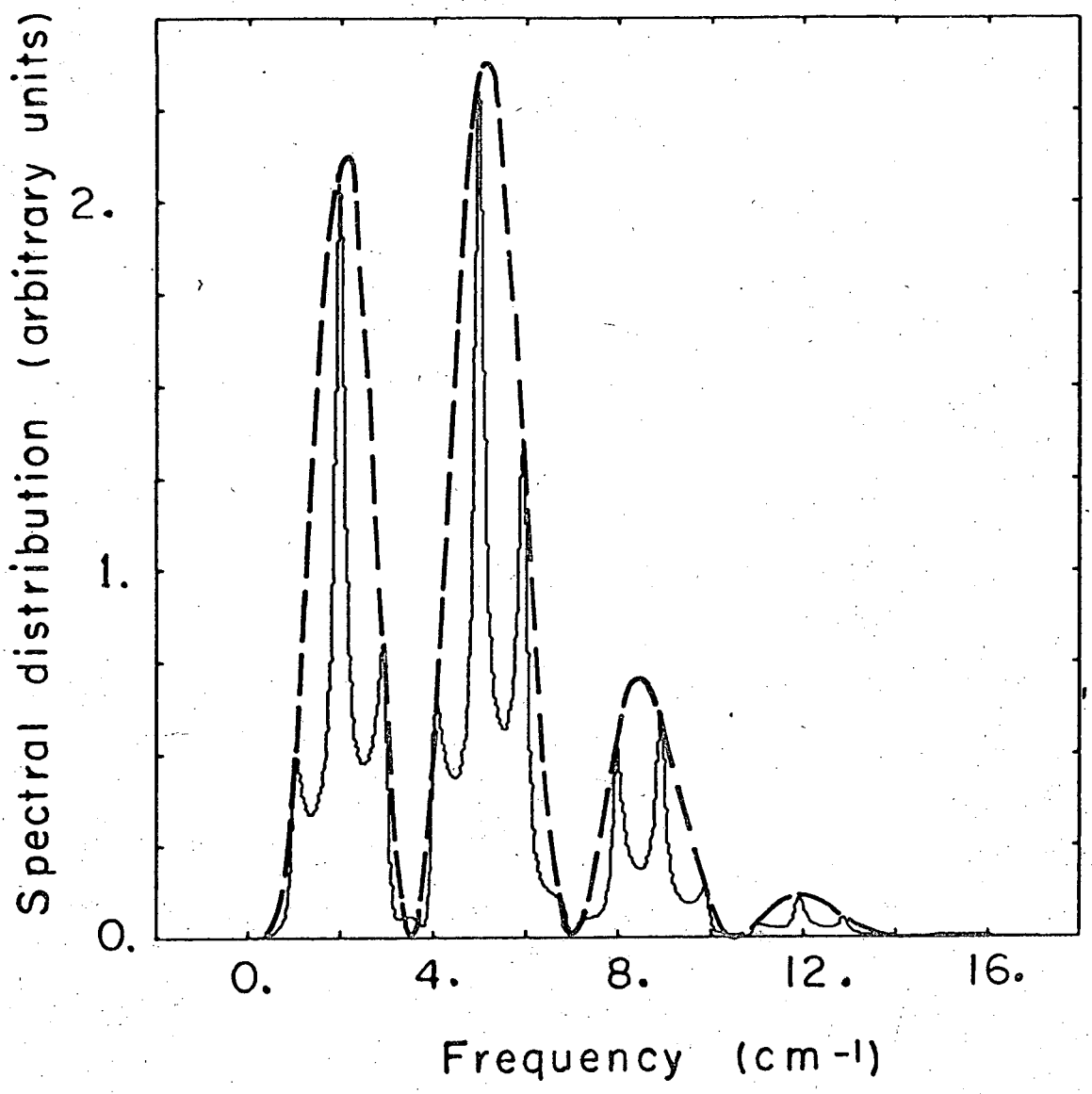

XBL709-3793

Fig. 1

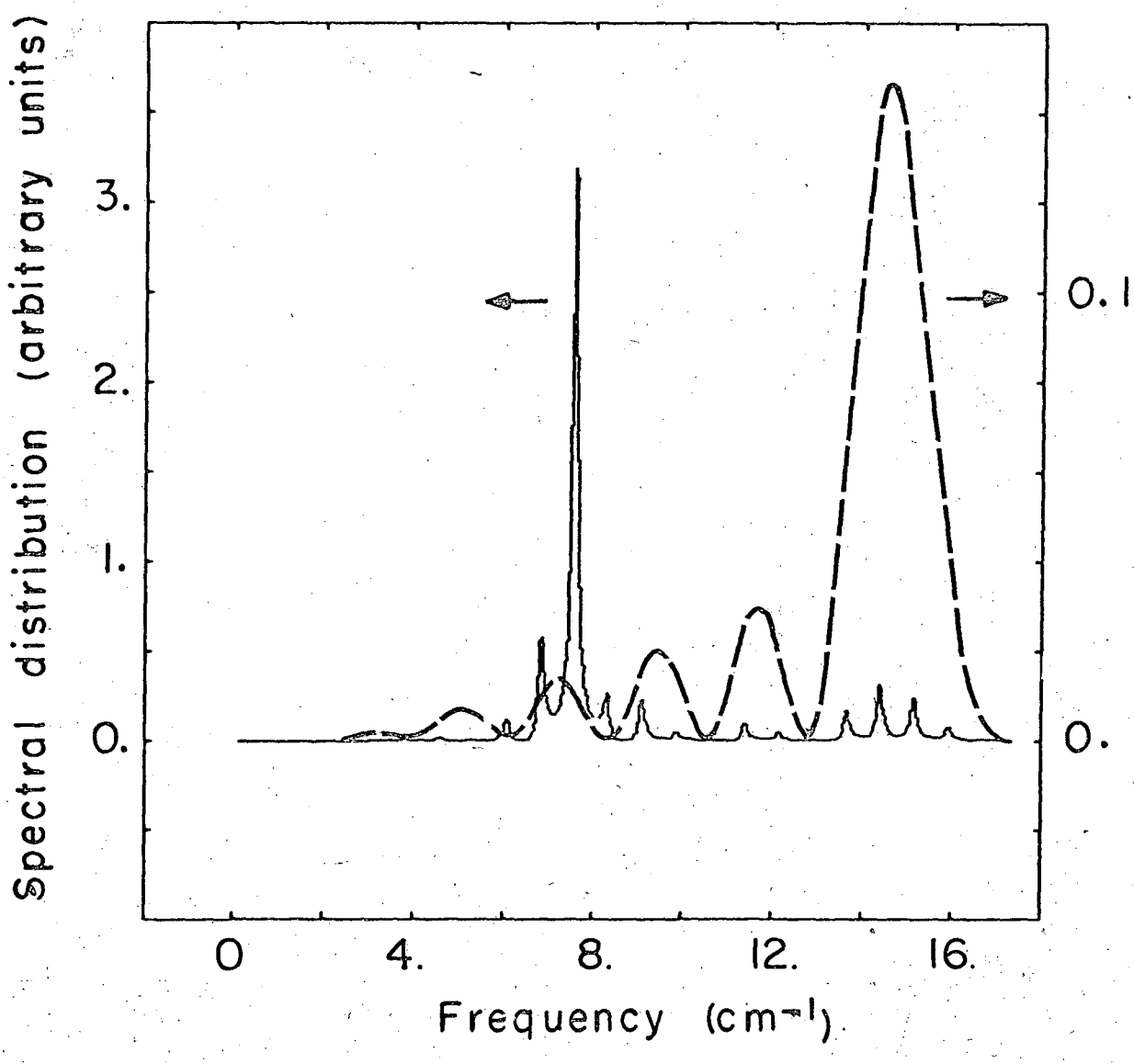

XBL709-3794

Fig. 2

LEGAL NOTICE

This report was prepared as an account of Government sponsored work. Neither the United States, nor the Commission, nor any person acting on behalf of the Commission:

A. Makes any warranty or representation, expressed or implied, with respect to the accuracy, completeness, or usefulness of the information contained in this report, or that the use of any information, apparatus, method, or process disclosed in this report may not infringe privately owned rights; or

B. Assumes any liabilities with respect to the use of, or for damages resulting from the use of any information, apparatus, method, or process disclosed in this report.

As used in the above, "person acting on behalf of the Commission" includes any employee or contractor of the Commission, or employee of such contractor, to the extent that such employee or contractor of the Commission, or employee of such contractor prepares, disseminates, or provides access to, any information pursuant to his employment or contract with the Commission, or his employment with such contractor.

TECHNICAL INFORMATION DIVISION
LAWRENCE RADIATION LABORATORY
UNIVERSITY OF CALIFORNIA
BERKELEY, CALIFORNIA 94720